J|A|C|S
JOURNAL OF THE AMERICAN CHEMICAL SOCIETY

Subscriber access provided by ISTANBUL TEKNIK UNIV

Article

Silicon/Molecule Interfacial Electronic Modifications

Tao He, Huanjun Ding, Naama Peor, Meng Lu, David A. Corley, Bo Chen, Yuval Ofir, Yongli Gao, Shlomo Yitzchaik, and James M. Tour

J. Am. Chem. Soc., **2008**, 130 (5), 1699-1710 • DOI: 10.1021/ja0768789

Downloaded from http://pubs.acs.org on February 8, 2009

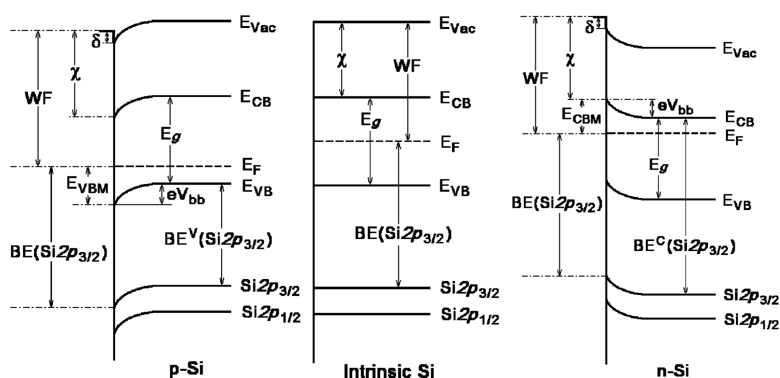

More About This Article

Additional resources and features associated with this article are available within the HTML version:

- Supporting Information
- Links to the 2 articles that cite this article, as of the time of this article download
- Access to high resolution figures
- Links to articles and content related to this article
- Copyright permission to reproduce figures and/or text from this article

View the Full Text HTML

ACS Publications
High quality. High impact.

Journal of the American Chemical Society is published by the American Chemical Society. 1155 Sixteenth Street N.W., Washington, DC 20036

J|A|C|S
ARTICLES
Published on Web 01/09/2008

Silicon/Molecule Interfacial Electronic Modifications

Tao He,[†] Huanjun Ding,[‡] Naama Peor,[§] Meng Lu,[†] David A. Corley,[†] Bo Chen,[†] Yuval Ofir,[§] Yongli Gao,*[,‡] Shlomo Yitzchaik,*[,§] and James M. Tour*[,†]

Departments of Chemistry, Computer Science, Mechanical Engineering and Materials Science, and the Smalley Institute for Nanoscale Science and Technology, Rice University, Houston, Texas 77005, Department of Physics and Astronomy, University of Rochester, Rochester, New York 14627, and Department of Inorganic and Analytical Chemistry, The Hebrew University of Jerusalem, Jerusalem 91904, Israel

Received September 11, 2007; E-mail: ygao@pas.rochester.edu; sy@cc.huji.ac.il; tour@rice.edu

Abstract: Electronic structures at the silicon/molecule interface were studied by X-ray photoelectron spectroscopy, ultraviolet photoelectron spectroscopy, inverse photoemission spectroscopy, and Kelvin probe techniques. The heterojunctions were fabricated by direct covalent grafting of a series of molecules ($-C_6H_4-X$, with X = NMe_2, NH_2, NO_2, and Mo_6 oxide cluster) onto the surface of four types of silicon substrates (both n- and p-type with different dopant densities). The electronic structures at the interfaces were thus systematically tuned in accordance with the electron-donating ability, redox capability, and/or dipole moment of the grafted molecules. The work function of each grafted surface is determined by a combination of the surface band bending and electron affinity. The surface band bending is dependent on the charge transfer between the silicon substrate and the grafted molecules, whereas electron affinity is dependent on the dipole moment of the grafted molecules. The contribution of each to the work function can be separated by a combination of the aforementioned analytical techniques. In addition, because of the relatively low molecular coverage on the surface, the contribution from the unreacted H-terminated surface to the work function was considered. The charge-transfer barrier of silicon substrates attached to different molecules exhibits a trend analogous to surface band bending effects, whereas the surface potential step exhibits properties analogous to electron affinity effects. These results provide a foundation for the utilization of organic molecule surface grafting as a means to tune the electronic properties of semiconductors and, consequently, to achieve controllable modulation of electronic characteristics in small semiconductor devices at future technology nodes.

Introduction

Inorganic semiconductor surfaces terminated with organic molecules have been studied extensively.[1−20] The potential advantages of using organic or organometallic molecules result from the versatility in offering a wide range of possibilities to tailor chemical and physical properties of materials and/or device characteristics. Moreover, molecular interfaces with semiconductors are rich in their behavior due to the variety of possible band structures and the potential for controlling the properties via doping and/or photoexcitation. The density and energy distribution of surface states, the surface electron affinity, and the chemical properties of surfaces can be controllably modulated via semiconductor surface engineering and thereby the device performance can be tuned. And the electronic structure of interfaces is dependent on the electronic properties of the

† Rice University.
‡ University of Rochester.
§ The Hebrew University of Jerusalem.

(1) Ashkenasy, G.; Cahen, D.; Cohen, R.; Shanzer, A.; Vilan, A. *Acc. Chem. Res.* **2002**, *35*, 121−128.
(2) Bocharov, S.; Dmitrenko, O.; De Leo, L. P. M.; Teplyakov, A. V. *J. Am. Chem. Soc.* **2006**, *128*, 9300−9301.
(3) Boulas, C.; Davidovits, J. V.; Rondelez, F.; Vuillaume, D. *Phys. Rev. Lett.* **1996**, *76*, 4797−4800.
(4) Buriak, J. M. *Chem. Rev.* **2002**, *102*, 1271−1308.
(5) Cahen, D.; Naaman, R.; Vager, Z. *Adv. Funct. Mater.* **2005**, *15*, 1571−1578.
(6) Cohen, R.; Ashkenasy, G.; Shanzer, A.; Cahen, D. Grafting Molecular Properties onto Semiconductor Surfaces. In *Semiconductor Electrodes and Photoelectrochemistry*; Bard, A. J., Stratmann, M., Licht, S., Eds.; Wiley: Weinheim, 2002, 127.
(7) Cohen, R.; Zenou, N.; Cahen, D; Yitzchaik, S. *Chem. Phys. Lett.* **1997**, *279*, 270−274.
(8) Cohen, R.; Kronik, L.; Vilan, A.; Shanzer, A.; Rosenwaks, Y.; Cahen, D. *Adv. Mater.* **2000**, *12*, 33−37.
(9) Deutsch, D.; Natan, A.; Shapira, Y.; Kronik, L. *J. Am. Chem. Soc.* **2007**, *129*, 2989−2997.
(10) Hunger, R.; Jaegermann, W.; Merson A.; Shapira Y.; Pettenkofer, C.; Rappich, J. *J. Phys. Chem. B* **2006**, *110*, 15432−15441.
(11) Quek, S. Y.; Neaton, J. B.; Hybertsen, M. S.; Kaxiras, E.; Louie, S. G. *Phys. Rev. Lett.* **2007**, *98*, 066807.
(12) Segev, L.; Salomon, A.; Natan, A.; Cahen, D.; Kronik, L. *Phys. Rev. B* **2006**, *74*, 165323.
(13) Yoder, N. L.; Guisinger, N. P.; Hersam, M. C.; Jorn, R.; Kaun, C. C.; Seideman, T. *Phys. Rev. Lett.* **2006**, *97*, 187601.
(14) Linford, M. R.; Fenter, P.; Eisenberer, P. M.; Chidsey, C. E. D. *J. Am. Chem. Soc.* **1995**, *117*, 3145−3155.
(15) Saito, N.; Hayashi, K.; Sugimura, H.; Takai, O. *Langmuir* **2003**, *19*, 10632−10634.
(16) Hurley, P. T.; Nemanick, E. J.; Brunschwig, B. S.; Lewis, N. S. *J. Am. Chem. Soc.* **2006**, *128*, 9990−9991.
(17) Vilan, A.; Ghabboun, J.; Cahen, D. *J. Phys. Chem. B* **2003**, *107*, 6360−6376.
(18) Bansal, A.; Li, X. L.; Lauermann, I.; Lewis, N. S.; Yi, S. I.; Weinberg, W. H. *J. Am. Chem. Soc.* **1996**, *118*, 7225−7226.
(19) Webb, L. J.; Lewis, N. S. *J. Phys. Chem. B* **2003**, *107*, 5404−5412.
(20) de Villeneuve, C. H.; Pinson, J.; Bernard, M. C.; Allongue, P. *J. Phys. Chem. B* **1997**, *101*, 2415−2420.

semiconductor substrate and the grafted molecules, the molecule−substrate bonding patterns, the molecular orientation, the surface coverage, and the molecular geometric structure requirements. If these various parameters can be better understood and tuned, then enormous semiconductor variability can be attained.

Prior work has been focused on understanding the Si/molecule interfaces.[5−13] If the molecule is chemisorbed directly on the surface, then the molecular energy levels are broadened significantly by the strong hybridization with the delocalized silicon wavefunctions, making it possible to transfer fractional amounts of charge to or from the molecule. A dipole-induced dielectric response for an adsorbed single polar molecule and/or the intermolecular dipole−dipole interactions for an adsorbed monolayer can cause depolarization and charge redistribution within the system. All of these may change the density and energy distribution of surface states and, thus, the surface band bending. The dipole contribution from the polar adsorbate can also alter the surface electron affinity. The changes in surface band bending and/or electron affinity will result in a change in work function of the investigated surface.

A specific motivation for the present study is provided by our recent work[21] in which the channel conductance in silicon devices were systematically modulated by the electron-donating ability of the molecules grafted atop oxide-free H-passivated silicon surfaces. Similarly, a higher conductivity in n-Si was observed using conductive atomic force microscopy (C-AFM) when the surface was covalently bonded to phenylacetylene.[15] The modulation in conductance was ascribed to the charge transfer between the device channel and the attached molecules during the grafting process. In our previous work, the device layer was nearly intrinsic p-Si (>2000 Ω cm) and a silicon oxide dielectric layer was present between the device and handle layers; therefore, it was difficult to do the characterizations directly on the devices in order to determine the charge transfer (except for the current−voltage measurements that were reported) because a good electrical connection is required for these techniques. In the present contribution, therefore, both p- and n-Si with different dopant densities were used as solid supports, and electronic structures of the Si/molecule interface were elucidated by means of ultraviolet photoelectron spectroscopy (UPS) and inverse photoemission spectroscopy (IPES) combined with X-ray photoelectron spectroscopy (XPS). A major advantage of the combination of the UPS/IPES and XPS analytical techniques is that the contributions due to band bending and change in electron affinities (i.e., surface dipoles) could be separated and, thus, complete equilibrium band energy diagrams could be developed.[10,22] In addition, the Kelvin probe technique was also used to identify the electronic states that define the energy levels. Regardless of the substrates, the molecular effect trends on the work function, surface band bending, and electron affinity are consistent in this work, as well as for the devices we have previously reported.[21] Unless stated otherwise, in the present contribution, we use the sign convention that all parameters are positive quantities.

Scheme 1. Molecular Structures of the Starting Molecules **1**−**4** Used for Grafting onto the Silicon Substrates[a]

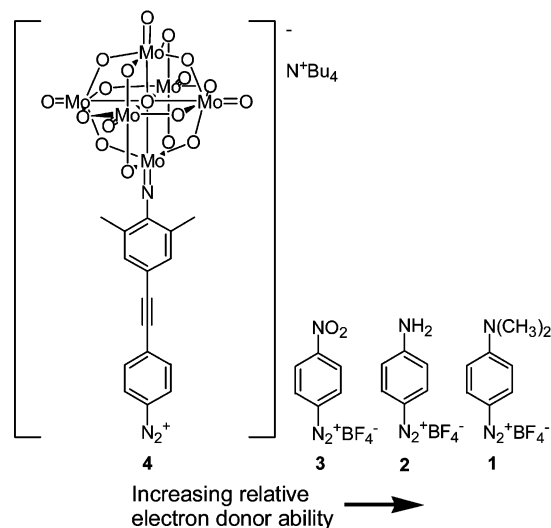

[a] Compound **1** is the most electron rich system due to the dimethylamino substituent, **2** is slightly lower in its electron donation capability, followed by **3** with its electron withdrawing nitro moiety and finally **4** bears an extremely electropositive polymolybdate.

Experimental Section

Materials. Anhydrous acetonitrile (CH_3CN, 99.5+%) for surface reactions was purchased from Sigma-Aldrich packed under nitrogen in a SureSeal container. CH_3CN, acetone (CH_3COCH_3), and isopropanol ($(CH_3)_2CHOH$) used for rinsing were HPLC grade and used without further purification. Concentrated sulfuric acid (H_2SO_4), concentrated hydrochloric acid (HCl), concentrated ammonium hydroxide (NH_4OH), 49% hydrofluoric acid (HF), and 30% hydrogen peroxide (H_2O_2) were reagent grade. Buffered-oxide etch (BOE, 10:1) was CMOS grade from J. T. Baker. The syntheses of the diazonium salts **1**−**4** (Scheme 1) were reported previously.[21,23−26] In the diazonium forms, they are thermally sensitive materials and were stored in the freezer prior to being used for molecular grafting.

Substrate Cleaning. Four types of silicon substrates with the <100> orientation (Virginia Semiconductor, Inc.) were used for molecular grafting: highly doped p-Si (HD-p-Si, B dopant, 0.01∼0.1 Ω cm, $0.28{\sim}8.49 \times 10^{18}$ cm^{-3}), moderately doped p-Si (MD-p-Si, B dopant, 3∼6 Ω cm, $0.46{\sim}2.25 \times 10^{15}$ cm^{-3}), highly doped n-Si (HD-n-Si, As dopant, < 0.0045 Ω cm, > 1.40×10^{19} cm^{-3}), and moderately doped n-Si (MD-n-Si, P dopant, 1 ∼ 10 Ω cm, $0.44{\sim}4.86 \times 10^{15}$ cm^{-3}). The wafers were cut into small shards and were cleaned consecutively under sonication for 10 min in acetone, isopropanol, and Milli-Q water, followed by rinsing copiously with Milli-Q water. They were then heated for 20 min in Piranha solution (98% H_2SO_4:H_2O_2, 7:3, v/v) at 85 °C (*CAUTION: strong oxidizing solution, handle with extreme care*). After etching in 2% HF solution for 1 min, the substrates were cleaned using the RCA protocol, i.e., they were treated in a mixture of NH_4OH (25%):H_2O_2 (30%):H_2O (1:1:5 v/v) at 70 °C for 10 min in order to remove organic surface films by oxidation. After a subsequent rinsing with Milli-Q water, the shards were treated in a mixture of HCl (32%):H_2O_2 (30%):H_2O (1:1:5 v/v) at 70 °C for 10 min in order to remove metal ions (Al^{3+}, Fe^{3+}, and Mg^{2+}) that would form insoluble hydroxides through reaction with NH_4OH. This acidic treatment also removed other metallic contaminants, such as gold, that were not removed by the basic

(21) He, T.; He, J. L.; Lu, M.; Chen, B.; Pang, H.; Reus, W. F.; Nolte, W. M.; Nackashi, D. P.; Franzon, P. D.; Tour, J. M. *J. Am. Chem. Soc.* **2006**, *128*, 14537−14541.
(22) Jaegermann, W. The Semiconductor/Electrolyte Interface: A Surface Science Approach. In *Modern Aspects of Electrochemistry*; White, R. E., Conway, B. E., Bockris, J. O. M., Eds.; Plenum Press: New York, 1996; Vol. 30.
(23) Becker, H. G. O.; Grossmann, K. *J. Prakt. Chem.* **1990**, *332*, 241−250.
(24) Milz, H.; Schladetsch, H. J. *Monodiazotization of Aromatic Diamines*; Ger. Offen., 1977; 15 pp.
(25) Dai, M. J.; Liang, B.; Wang, C. H.; Chen, J. H.; Yang, Z. *Org. Lett.* **2004**, *6*, 221−224.
(26) Lu, M.; Nolte, W. M.; He, T.; Corley, D. A.; Tour, J. M., to be submitted.

treatment. The silicon substrates were then rinsed using Milli-Q water and dried by N_2 flow.

Molecular Grafting. The molecules **1**−**4** were directly grafted onto the silicon surface using the previously reported method.[21,26,27] Before molecular grafting, the as-cleaned silicon shards were etched in an Ar-purged BOE for 5 min to remove the SiO_x layer and form the H-passivated silicon surface. The grafting process was carried out by exposing the freshly etched samples to a 0.5 mM solution of the diazonium salt (**1**−**4**) in anhydrous CH_3CN in the dark under an inert atmosphere. The grafting time was carefully calibrated for monolayer formation, depending on the molecule and its concentration. The grafting time was 5 h for compound **1**, 45 min for compounds **2** and **3**, and 2 h for compound **4**.[21,26] After the molecular grafting, the samples were rinsed thoroughly with CH_3CN to remove the residual diazonium salt and the physisorbed materials, and then dried with a N_2 flow. The ellipsometric thicknesses of the molecular thin films were consistent with the theoretical lengths of the grafted molecules, indicating that a molecular monolayer was formed on the silicon surface.

Ellipsometry. Molecular layer thicknesses were monitored with a single-wavelength (632.8-nm laser) LSE Stokes ellipsometer (Gaertner Scientific) with an incident angle of 70°. Ellipsometric characterizations were carried out before and immediately after monolayer preparation. The surface thickness was modeled as a single adsorbing layer atop an infinitely thick substrate. The index of refraction (n_f) was set at 1.50 and 0 for extinction coefficient (k_f). The thickness was the average value of the measured results at three different locations for each sample.

X-ray Photoelectron Spectroscopy (XPS). XPS data were collected at room temperature using a PHI 5700 XPS/ESCA system (PHI Quantera SXM Scanning X-ray Microprobe) equipped with a monochromatic Al $K\alpha$ light source (1486.6 eV) at a takeoff angle of 45°. All samples were transferred to the ultrahigh vacuum (UHV) chamber ($\sim 10^{-9}$ Torr) within 20 min after the molecular grafting. No signal from SiO_x was observed when the samples were kept in air for 30−60 min after BOE etching, indicating the H-passivated surface is relatively stable in the presence of oxygen and humidity.[27−29] The analytical spot size for all measurements was 0.10 mm × 0.10 mm. Unless stated otherwise, the measurements were done with a pass energy of 6.5 eV. The data were analyzed using the MultiPak Spectrum software, V7.01.

Ultraviolet Photoelectron Spectroscopy (UPS) and Inverse Photoemission Spectroscopy (IPES). Photoemission spectroscopy of occupied and unoccupied states of the system was performed using a VG ESCA Lab system equipped with both UPS and IPES. The spectrometer chamber of the UHV system had a base pressure of 8×10^{-11} Torr. Occupied states (or valence band) spectra were obtained by UPS using the unfiltered He I line (21.2 eV) of a discharge lamp with the samples biased at −5.0 V to avoid the influence of the detector work function and to observe the true low-energy secondary cutoff. The typical instrumental resolution for UPS measurements ranges from ∼0.03 to 0.1 eV with photon energy dispersion of less than 20 meV. Unoccupied states (or conduction bands) were measured by IPES using a custom-made spectrometer composed of a commercial Kimball Physics ELG-2 electron gun and a bandpass photon detector prepared according to an existing design.[30−32] IPES was done in the isochromat mode using a photon detector centered at a fixed energy of 9.8 eV. The combined resolution (electron + photon) of the IPES spectrometer was determined to be ∼0.6 eV from the width of the Fermi edge measured on a clean polycrystalline Au film. The UPS and IPES energy scales were aligned by measuring the position of the Fermi level on a freshly evaporated Au film. The position of the vacuum level, E_{vac}, was measured for each surface using the onset of the secondary cutoff in the UPS spectra. All the measurements were done at room temperature.

(27) Stewart, M. P.; Maya, F.; Kosynkin, D. V.; Dirk, S. M.; Stapleton, J. J.; McGuiness, C. L.; Allara, D. L.; Tour, J. M. *J. Am. Chem. Soc.* **2004**, *126*, 370−378.
(28) Hines, M. A.; Chabal, Y. J.; Harris, T. D.; Harris, A. L. *J. Chem. Phys.* **1994**, *101*, 8055−8072.
(29) Hines, M. A. *Annu. Rev. Phys. Chem.* **2003**, *54*, 29−56.
(30) Yan, L.; Watkins, N. J.; Zorba, S.; Gao, Y. L.; Tang, C. W. *Appl. Phys. Lett.* **2001**, *79*, 4148−4150.
(31) Ding, H. J.; Gao, Y. L. *Appl. Phys. Lett.* **2005**, *86*, 213508.
(32) Ding, H. J.; Zorba, S.; Gao, Y. L.; Ma, L. P.; Yang, Y. *J. Appl. Phys.* **2006**, *100*, 113706.

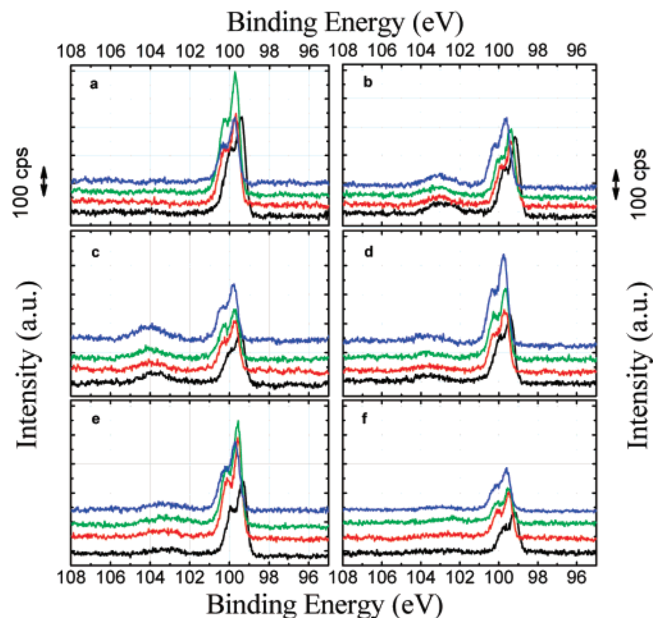

Figure 1. Typical XPS core-level spectra of Si2*p* measured on different systems. (a) H-terminated silicon substrates (Si−H); (b) with the presence of SiO_x on the silicon surfaces; silicon substrates were grafted by (c) **1** (Si−NMe_2); (d) **2** (Si−NH_2); (e) **3** (Si−NO_2), and (f) **4** (Si−Mo). Black line (on bottom in each spectrum): HD-p-Si substrate; red line (second from bottom in each spectrum): MD-p-Si substrate; green line (second from top in each spectrum): MD-n-Si substrate; blue line (top line in each spectrum): HD-n-Si substrate.

Kelvin Probe. The Kelvin probe method is widely used to determine the relative work function of metals and semiconductors by measuring the contact potential difference (CPD) between a reference surface and a sample; this analytical method is sensitive and does not disturb the surface state of the sample under test.[33−35] The measurements were performed using a commercial Kelvin probe S (Besocke Delta-Phi, Jülich, Germany), as part of a home-built setup, in the ambient inside a N_2-filled glovebox. A vibrating gold grid (3 mm in diameter) was used as the reference electrode (work function 5.1 eV). A high-intensity white illumination of ∼200 mW/cm^2 was obtained from a quartz tungsten-halogen (QTH) lamp for the photosaturation experiments. The sample and probe were put in a Faraday cage to minimize electrical interference from external sources.

Results

(a) XPS. XPS is a surface analysis technique that measures the chemical states and electronic states of the elements that exist within a material. XPS binding energy (BE) is a property of the hole state produced by removal of the core electron, which can be affected by the charge transfer by virtue of the Coulomb potential produced within the atom by the gain or loss of charge by outer orbitals. Figure 1 shows the representative detailed XPS spectra of the Si2*p* core level for silicon substrates grafted with different molecules. H-terminated silicon samples (Si−H) prepared by BOE etching were used as the reference. Silicon with a SiO_x layer on the surface was used as the control sample

(33) Kronik, L.; Shapira, Y. *Surf. Sci. Rep.* **1999**, *37*, 1−206.
(34) Ruhle, S.; Cahen, D. *J. Appl. Phys.* **2004**, *96*, 1556−1562.
(35) Ofir, Y.; Zenou, N.; Goykhman, I.; Yitzchaik, S. *J. Phys. Chem. B* **2006**, *110*, 8002−8009.

and was prepared by heating the as-etched silicon in a mixed solution of H_2SO_4 and H_2O_2 or in a mixture of H_2O_2, NH_4OH, and H_2O. The oxide thickness was about 2 nm. The strong peak around 99.5 eV (Figure 1) corresponds to the signal from bulk silicon (Si^0+SiH), whereas the broad peak around 103 eV results from the SiO_x.[36] For the Si−H reference, there was no SiO_x present (Figure 1a). After the samples had been molecularly grafted, although the grafting process was done under a N_2 atmosphere inside a glove box, XPS indicated that various small amounts of SiO_x were present due to the extended handling (Figure 1c-f).

(b) UPS/IPES. UPS is a useful method for probing the electronic structures of material surfaces. Figure 2 is the UPS spectra of different molecular systems in which both the low-energy secondary cutoff and the highest occupied molecular orbital (HOMO) region (or valence band) are shown in BE relative to the Fermi level. The sharp intensity drop in the UPS spectra for BE around 17 eV is the so-called secondary electron edge (cutoff region), which corresponds to the energy level at which the photons are unable to eject electrons with any greater BE. Its energy position (E_{cutoff}) is extracted according to the on-set edge in the UPS spectra (Figure 2B). Thus, the work function (WF_{UPS}) of the investigated surface can be determined according to eq 1. The energy for the photon ($h\nu$) is 21.2 eV. The HOMO level is determined directly using the on-set edge in the spectra (Figure 2C) instead of the peak value. The values of E_{cutoff}, WF_{UPS}, and HOMO for different systems are shown in Table 1. Similarly, the on-set edge in IPES spectrum was used to extract the lowest unoccupied molecular orbital (LUMO) level of the Si−H reference (Table 2).

$$WF_{UPS} = h\nu - E_{cutoff} \quad (1)$$

eV_{bb}, surface band bending; χ, electron affinity; E_{VBM}, charge-transfer barrier for holes; E_{CBM}, charge-transfer barrier for electrons; BE(Si*2p3/2*), binding energy of Si*2p3/2* with respect to the Fermi level (E_F); BE^V(Si*2p3/2*), binding energy of Si*2p3/2* with respect to the valence band maximum (E_{VB}) in the bulk silicon; BE^C(Si*2p3/2*) binding energy of Si*2p3/2* with respect to the conduction band minimum (E_{CB}) in the bulk silicon.

(c) Kelvin Probe. The Kelvin probe method was another technique that was used to determine the work function (WF_{CPD}), band bending (BB_{CPD}), and electron affinity (χ_{CPD}) of the studied surface by measuring the CPD in the dark (CPD_D) and under photosaturation (CPD_L). CPD_D is the value for the case in thermal equilibrium, from which the WF_{CPD} can be calculated according to eq 2 using a 5.1-eV work function of the probe (WF_{KP}). For a metal-semiconductor arrangement, electrons and holes are generated next to the surface when the Si sample is illuminated, while the work function of the metallic probe does not change under illumination. For n-type semiconductors, the photogenerated electrons move toward the Si bulk being driven by the built-in electric field at the surface, whereas holes move toward the surface where they recombine with trapped electrons in surface states. For p-type semimconductors, the photogenerated holes move toward the Si bulk, while electrons move toward the surface where they recombine with trapped positive charges in surface states. This induces the charge redistribution in the space charge region and at the surface and, accordingly,

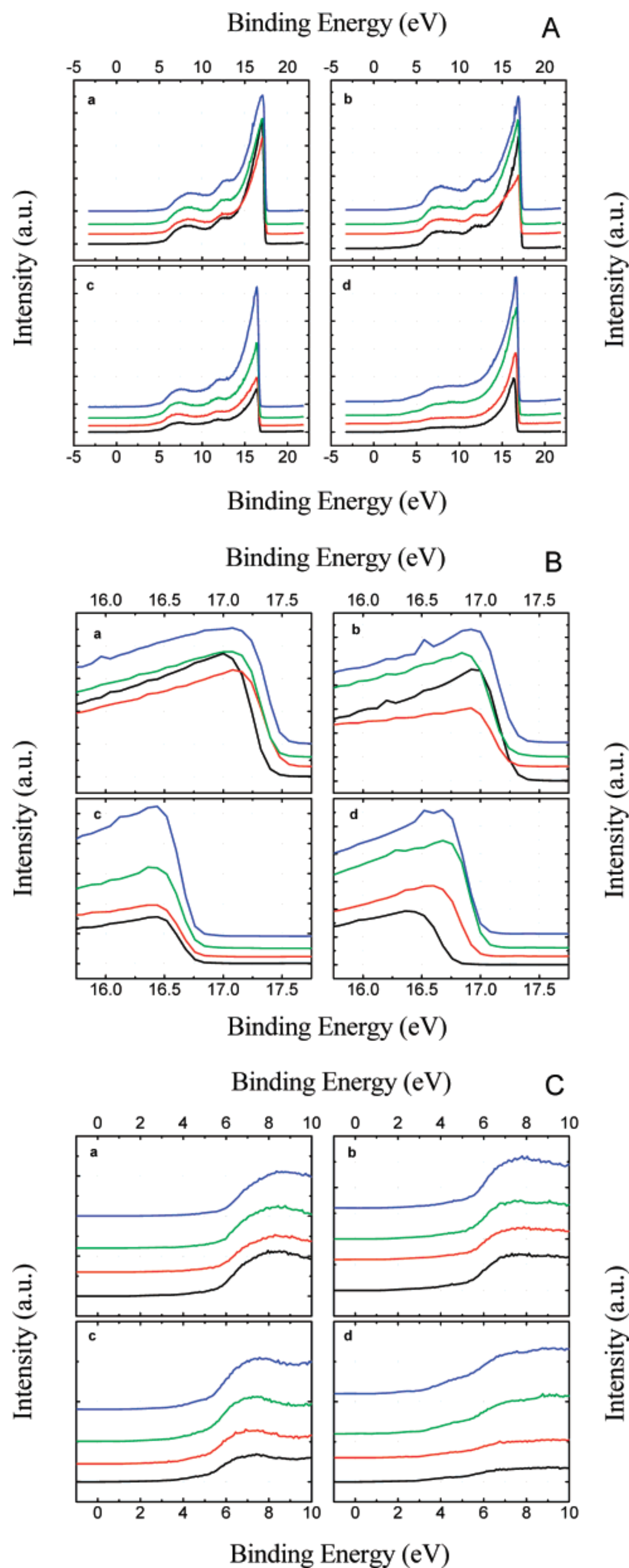

Figure 2. Representative UPS spectra measured on different systems: (A) Survey; (B) Cut-Off; and (C) HOMO. Silicon substrates were grafted by (a) **1** (Si−NMe_2), (b) **2** (Si−NH_2), (c) **3** (Si−NO_2), and (d) **4** (Si−Mo). The black line (on bottom in each spectrum): HD-p-Si substrate; red line (second from bottom in each spectrum): MD-p-Si substrate; green line (second from top in each spectrum): MD-n-Si substrate; blue line (top in each spectrum): HD-n-Si substrate.

the change in electrical potential distribution. The bands at the surface are thus flattened in an ideal case of photosaturation

(36) Shallenberger, J. R. *J. Vac. Sci. Technol. A* **1996**, *14*, 693−698.

Table 1. Energy Levels (eV) of E_{cutoff}, WF_{UPS}, and HOMO for Different Systems Determined from UPS Data

	Si-Mo				$Si-NO_2$				$Si-NH_2$				$Si-NMe_2$			
	HD-p-Si	MD-p-Si	MD-n-Si	HD-n-Si	HD-p-Si	MD-p-Si	MD-n-Si	HD-n-Si	HD-p-Si	MD-p-Si	MD-n-Si	HD-n-Si	HD-p-Si	MD-p-Si	MD-n-Si	HD-n-Si
E_{cutoff}	16.67	17.31	16.91	16.88	16.54	16.58	16.62	16.56	17.09	17.09	17.12	17.16	17.31	17.48	17.40	17.49
WF_{UPS}	4.53	4.39	4.29	4.32	4.66	4.62	4.58	4.64	4.11	4.11	4.08	4.04	3.89	3.72	3.80	3.71
HOMO	1.25	1.31	1.40	1.39	1.39	1.38	1.43	1.46	1.42	1.45	1.46	1.51	1.67	1.72	1.77	1.81

Table 2. Energy Levels (eV) for the Si−H Control Samples Derived from the Combination of UPS/IPES and XPS Data

	E_{cutoff}	WF_{UPS}	HOMO	LUMO	BE($Si2p_{3/2}$)	eV_{bb}	χ	E_{VBM}	E_{CBM}	$BE^V(Si2p_{3/2})$	$BE^C(Si2p_{3/2})$
HD-p-Si	16.65	4.55	0.78	0.8	99.47	0.71	4.23	0.78		98.69	
MD-p-Si	16.99	4.21	1.01	0.6	99.71	0.75	4.11	1.01		98.73	
MD-n-Si	16.96	4.24	1.08	0.6	99.71	0.34	3.68		0.59		100.30
HD-n-Si	16.90	4.30	1.11	0.5	99.77	0.48	3.80		0.50		100.27

illumination. The electron affinity can be determined subsequently.

$$WF_{CPD} = WF_{KP} + CPD_D \quad (2)$$

Discussion

(a) Shift in Si2*p* Core Level after Molecular Grafting. Although the absolute value of binding energy (BE) may be questioned, the present samples provide an internally consistent set for relative comparisons, which is preferred for fine analysis. The discussion below relies, therefore, on differences among the samples, i.e., on the shift in peak of Si2*p* bulk spectra. To obtain this shift after surface modification, a careful deconvolution was done on the Si2*p* bulk spectra. The fit criterion is that the branching ratio of Si2*p3/2* to Si2*p1/2* is 2:1. A fixed 90% Gaussian−10% Lorentzian ratio was used for every band fitting. After deconvolution, a doublet split of 0.61 ± 0.01 eV was thereby calculated, reflecting the spin orbit splitting of the 2*p* shell, and it was comparable to the literature value (~0.60 eV).[37,38] A value of 0.52−0.58 eV for the full width at half-maximum (fwhm) of Si2*p3/2* was calculated, for which the literature value is 0.48−0.52 on annealed wafers[37,38] and 0.60−0.75 eV on as-implanted wafers.[38] The BE peak positions of both Si2*p3/2* and Si2*p1/2* are observed in the series Si−Mo < $Si-NO_2$ < $Si-NH_2$ < $Si-NMe_2$ (Figure 3), which follows the electron donor ability of the chemical species attached on the silicon surface. That is, the sample grafted with strong electron-donating molecules (e.g., $Si-NMe_2$) has a higher peak value of Si2*p* core level, whereas the strong electron-withdrawal sample (e.g., Si−Mo) has the lowest peak value. In addition, the silicon covered by oxides was observed to exhibit an even lower peak value of Si2*p* core level than Si−Mo. To make consistent comparisons, the peak value of the Si2*p* core level for the H-terminated silicon sample was used as the reference (Table 2) with excellent repeatability; the standard deviation for the samples with different silicon substrates was between ±0.02 and ±0.05 eV for Si2*p3/2* and between ±0.03 and ±0.05 eV for Si2*p1/2*. The shift of the Si2*p* bulk spectrum is thus calculated by subtracting the reference value from the sample value (shift value = Si2*p3/2*(sample) − Si2*p3/2*(reference), Figure 4), indicating a trend that parallels the electron donor ability of the molecules grafted on the surface. Moreover, the trend in these molecular effects is independent of the silicon type and doping density of the solid support albeit with different values for different substrates (Figures 3 and 4). Here, one should note that the reference for the extraction of core level shift is the sample with both Si^0 and SiH rather than with Si^0 itself, which explains why the value of the core level shift is not always positive for some donor systems.

The observed molecular effects are consistent with the fact that highly doped n-Si has the highest BE in Si2*p* bulk spectra, and highly doped p-Si exhibits the lowest BE (Figures 3 and 4). The electron-donating molecules therefore behave like a donor to silicon, for which the negative charge is donated to the lattice in the conduction band, which makes it more n-type. The electron-withdrawing molecules behave like an acceptor, in which the positive charge (hole) is created in the valence band and negative charge is gained by the grafted molecules, making the silicon more p-type. The impacts of molecular grafting on the core-level shift can be explained by the screening effects of negative charge in outer orbitals (conduction band) on the core hole. If there are more negative charges in the conduction band (donor-like molecules), it will take more energy (higher BE) to remove the core electron due to the screening effects; on the other hand, it will take less energy (lower BE) to remove the core electron in the case that more holes are present in the valence band (acceptor-like molecules). In addition, the Fermi level is located higher in the gap for n-doped than that of p-doped semiconductor. Because the Fermi level of the sample under test is aligned with that of the system during the XPS measurements, n-doped samples will have a larger BE (relative to the Fermi level). The more n-type, the higher BE becomes. To minimize the possibility that the results are caused by the influences of beam-induced degradation during the XPS measurements, two different pass energies, 6.5 and 26 eV, were used. The same trend was observed for Si2*p* (results are not shown here), though with different BE peak values. Therefore, even if there was degradation during the measurements, it does not affect the aforementioned conclusions drawn from the XPS results.

(b) Tailoring of the Work Function. As discussed previously, the work function of the sample under test can be measured using both UPS and Kelvin probe techniques.[39] The former gives a direct measure of the work function of the solid, and the latter gives a value relative to the work function of the probe itself. For clean and well-ordered Si crystal, in light of the doping concentration, the theoretical values of the work

(37) Shallenberger, J. R.; Cole, D. A.; Novak, S. W. *J. Vac. Sci. Technol. A* **1999**, *17*, 1086−1090.
(38) Shallenberger, J. R.; Cole, D. A. *1998 International Conference on Ion Implantation Technology Proceedings*, **1999**, 1, 566−569.

(39) Cahen, D.; Kahn, A. *Adv. Mater.* **2003**, *15*, 271−277.

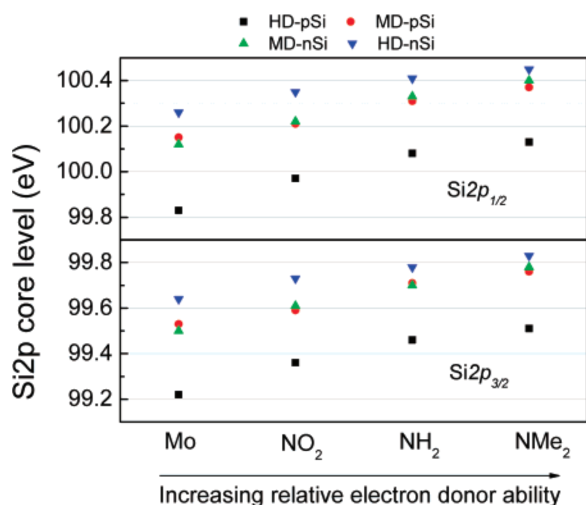

Figure 3. Peak positions on Si2*p* bulk spectra for different systems after molecular grafting. Note that the trend is substrate independent.

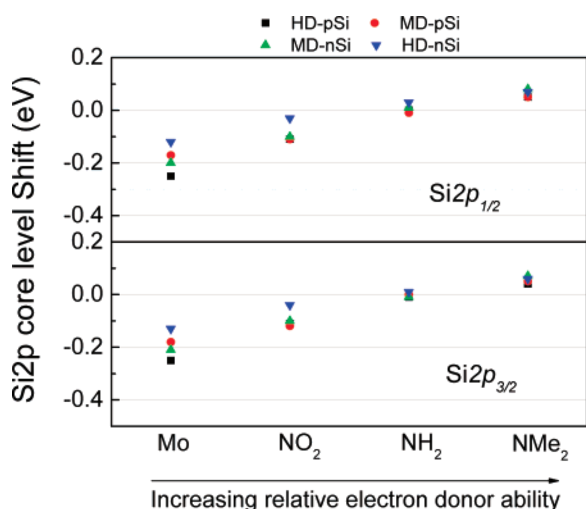

Figure 4. Shift in peak positions of Si2*p* bulk spectra derived from the data shown in Figure 3. Note that the trend is substrate independent.

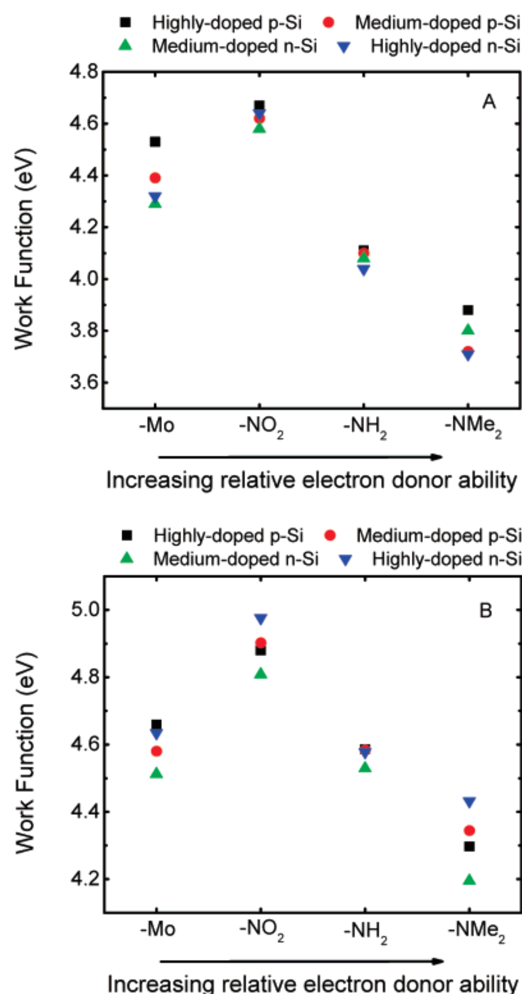

Figure 5. Work functions of the investigated surfaces derived from results of (A) UPS and (B) Kelvin probe measurements.

function for the bulk HD-p-Si, MD-p-Si, MD-n-Si, and HD-n-Si are calculated to be 5.098, 4.939, 4.302, and 4.065 eV, respectively. In the UPS spectrum, the work function of the investigated surface (WF_{UPS}) is the difference between the vacuum level ($E_{vac,UPS}$) and the energy of the electrons originating from the Fermi level of the sample, which is determined according to eq 1. In the case of Kelvin probe measurements, the work function of the studied surface (WF_{CPD}) is derived from eq 2. The values of work function from both UPS and Kelvin probe are presented in Figure 5. Using the H-terminated surface as the reference, similar to the analysis of the shift in Si2*p* core level, the change in work function of the investigated surfaces induced by molecular grafting is shown in Figure 6. An obvious trend in both the work function and its change is observed, although with different values, which agrees with the electron-donating ability of the grafted molecules. The most electron-rich system (**1**, Si$-$NMe$_2$) has the lowest work function, followed by the one with a slightly lower electron-donation capability (**2**, Si$-$NH$_2$); whereas the electron deficient system (**3**, Si$-$NO$_2$) has the highest work function. The work function of the investigated semiconductor surface is determined by three factors: (i) the energy difference between the Fermi level and conduction band minimum (E_{CB}) in the bulk; (ii) the surface band bending (eV_{bb}), the electrical potential difference between the surface and the electrically neutral semiconductor bulk, which is usually expressed in the band diagram by the bending of E_{VB} and E_{CB} near the surface; and (iii) the electron affinity (χ). Before molecular grafting (Si bulk), the difference between E_F and E_{VB} in the bulk for HD-p-Si and MD-p-Si is calculated to be 0.074 and 0.263 eV, respectively, whereas that between E_F and E_{CB} for MD-n-Si and HD-n-Si is 0.255 and 0.018 eV, respectively. For the samples under test, the ratio of atoms at the surface to those in the bulk is very small. Unlike impurity doping, even in the case that partial charges transfer between Si and the grafted molecules, the Fermi level in the bulk is not altered with different molecular attachments. Therefore, the change in work function induced by molecular grafting is attributed to the changes in eV_{bb} and χ, which are discussed in detail in the following sections. Note that the Si surface modified by the molecule that is the most electron withdrawing (**4**, Si$-$Mo) has a work function between Si$-$NO$_2$ and Si$-$NH$_2$, rather than the highest value among all the samples. This is different from the XPS results, in which the Si$-$Mo shows a stronger molecular effect than Si$-$NO$_2$. The reasons for this difference are discussed in the last section.

(c) Tailoring of Charge-Transfer Barrier and eV_{bb} Upon Molecular Grafting. Band bending is associated with the

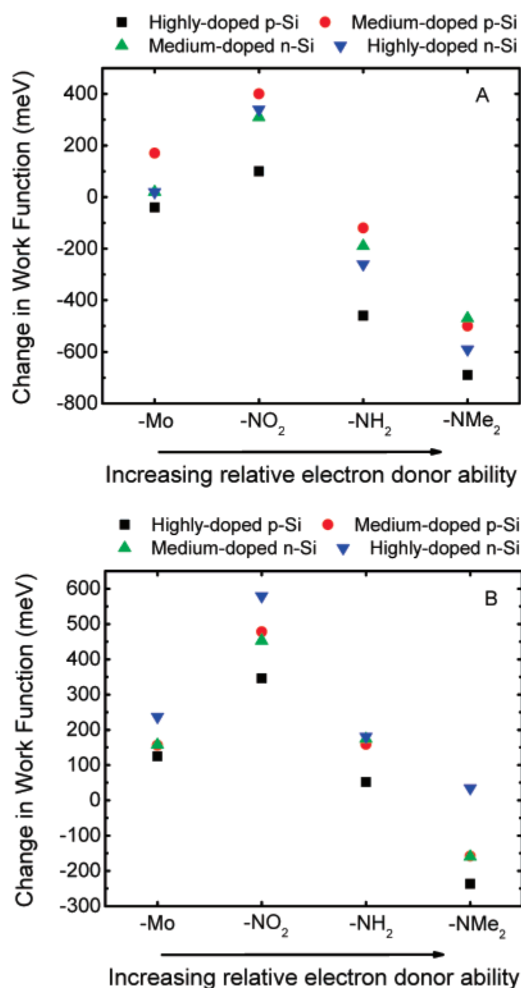

Figure 6. Change in work function of the investigated surfaces before and after molecular grafting using the Si−H surface as the reference, and derived from data shown in (A) Figure 5A and (B) Figure 5B.

surface states/traps, i.e., with the density and energy distribution of the surface charge. The charge-transfer takes place between the molecules and substrates as the molecules are grafted onto the surface due to the formation of chemical bonds, different Fermi levels between the substrates and grafted molecules, dipole moment effects, and so on. This charge transfer is dependent on its barrier, which is defined by the energy difference between the E_F and E_{VB} for holes (E_{VBM}, eq 3) and that between the E_F and E_{CB} for electrons (E_{CBM}, eq 4), as indicated in Figure 7. The lower the barrier, the easier is the charge transfer. Once the charge barrier is determined, the eV_{bb}, relating to the change in surface charge, can be calculated according to eqs 5 (holes) and 6 (electrons). The values of $(E_F - E_{VB})_{bulk}$ and $(E_{CB} - E_F)_{bulk}$ are presented in the previous section.

$$E_{VBM} = (E_F - E_{VB})_{surface} \quad (3)$$

$$E_{CBM} = (E_{CB} - E_F)_{surface} \quad (4)$$

$$eV_{bb} = E_{VBM} - (E_F - E_{VB})_{bulk} \quad (5)$$

$$eV_{bb} = E_{CBM} - (E_{CB} - E_F)_{bulk} \quad (6)$$

As shown in Figure 7, the Si2$p_{3/2}$ core level (BE(Si2$p_{3/2}$)) is determined relative to E_F in the XPS measurement, which varies with eV_{bb} of the sample. If the binding energy is derived with respect to E_{VB} for p-Si (BE^V(Si2$p_{3/2}$)) or with respect to E_{CB} for n-Si (BE^C(Si2$p_{3/2}$)), then it is constant and independent of eV_{bb}. If BE^V(Si2$p_{3/2}$) or BE^C(Si2$p_{3/2}$) is known, then the hole injection barrier (E_{VBM}) or electron injection barrier (E_{CBM}) for Si substrates modified with different molecules can thus be determined according to eqs 7 and 8, respectively, and, therefore eV_{bb} can also be determined. The H-terminated Si surface (Si−H) is used as a reference to obtain the BE^V(Si2$p_{3/2}$) for p-Si substrates and BE^C(Si2$p_{3/2}$) for n-Si. The BE(Si2$p_{3/2}$) for Si−H is determined from the XPS measurements while E_{VBM} for Si−H is derived from the UPS results, and E_{CBM} is from the IPES (Table 2). Thus, BE^V(Si2$p_{3/2}$) or BE^C(Si2$p_{3/2}$) for different substrates is obtained and shown in Table 2. BE^V(Si2$p_{3/2}$) is close to the literature value (98.74 eV).[10,40] Subsequently, E_{VBM} and E_{CBM} for the substrates grafted with different molecules are extracted, as shown in Figure 8.

$$E_{VBM} = BE(Si2p_{3/2}) - BE^V(Si2p_{3/2}) \quad (7)$$

$$E_{CBM} = BE^C(Si2p_{3/2}) - BE(Si2p_{3/2}) \quad (8)$$

For p-Si substrates (Figure 8), the most electron rich system (Si−NMe_2) has the highest hole injection barrier, followed by the one with a slightly lower electron-donation capability (Si−NH_2), then the electron deficiency system (Si−NO_2), whereas the most electron deficiency system (Si−Mo) has the lowest hole injection barrier. eV_{bb} for p-Si substrates is calculated according to eq 5, and the results are plotted in Figure 9. The same trend as that for E_{VBM} is observed. Si−NMe_2 has the highest eV_{bb}, followed by Si−NH_2, then Si−NO_2, and Si−Mo has the lowest eV_{bb}. Furthermore, the trend for both E_{VBM} and eV_{bb} is substrate independent. This agrees well with our previous observations in devices that the threshold voltage for a p-channel MOSFET increases with the increasing relative electron donor-ability of the molecules grafted in the channel region.[21] The higher the eV_{bb}, the stronger the depletion layer is on the surface. Therefore, among the samples grafted by molecules **1**−**4**, on p-Si substrates the Si−NMe_2 system has the strongest depletion in the surface region, followed by Si−NH_2, then Si−NO_2, and Si−Mo has the weakest depletion. This is reasonable since the depletion layer in p-Si is correlated with the positive surface charge (i.e., with the negative space charge of ionized acceptors). The electron donating molecules give electrons to the p-Si substrates and, thus, they become partly positively charged, leading to an increase in the positive surface charge density. Accordingly, the depletion becomes stronger. As expected, the opposite trend is seen for the electron withdrawing molecules.

The effect can also be viewed from the perspective of charge transfer. Some holes in the space charge region can recombine with the negative charges (electrons) donated by the electron donating molecules, resulting in lower hole density. Simultaneously, the negative charge density in the surface decreases by the same amount due to the transfer of negative charges from molecules to p-Si. Thus a stronger depletion in the space charge region is formed. When p-Si is modified by electron withdrawing molecules, some holes are created in the space charge region

(40) Himpsel, F. J.; Hollinger, G.; Pollak, R. A. *Phys. Rev. B* **1983**, *28*, 7014−7018.

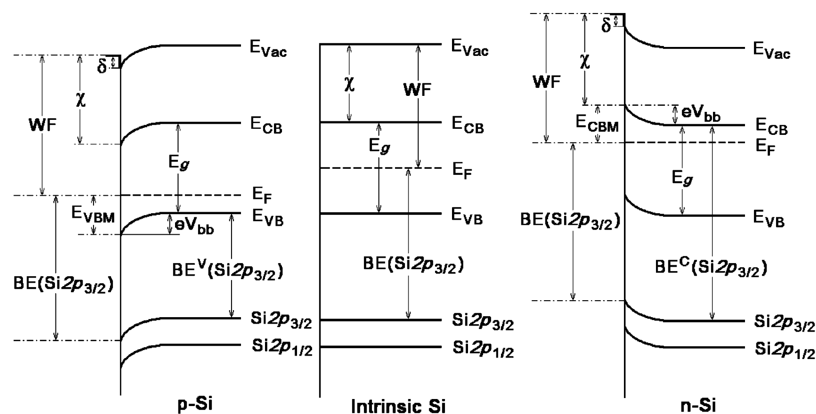

Figure 7. Energy band diagram of a silicon surface: functionalized p-Si, clean intrinsic Si, and functionalized n-Si. eV_{bb} is derived from the energy levels in the bulk silicon (Fermi level, E_F, valence band for p-Si, E_{VB}, and conduction band for n-Si, E_{CB}) and the measurement of the binding energy of Si2$p_{3/2}$ core level, which is measured relative to E_F using XPS. Surface potential step (δ), modifying the intrinsic χ of silicon, is determined from the WF measured using UPS and the eV_{bb}.

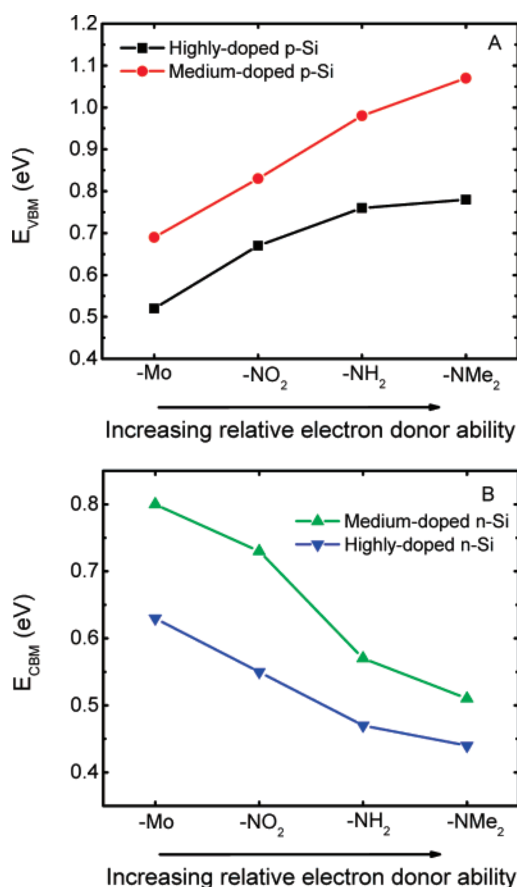

Figure 8. (A) Hole injection barrier (distance between E_{VB} and E_F) of different p-Si substrates grafted by a monolayer of **1**−**4**. (B) Electron injection barrier (distance between E_F and E_{CB}) of different n-Si substrates grafted by a monolayer of **1**−**4**. The results were derived from the combination of XPS and UPS/IPES results.

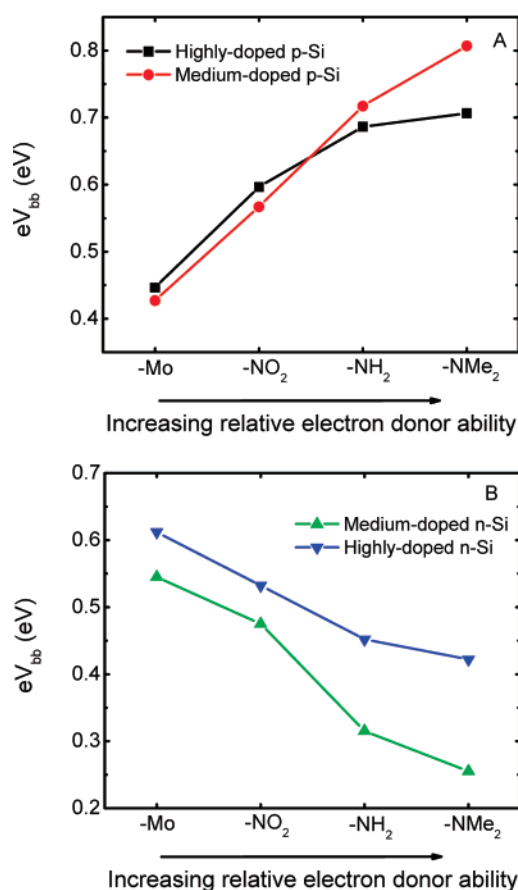

Figure 9. (A) eV_{bb} for p-Si substrates grafted by a monolayer of **1**−**4**, derived from the data shown in Figure 8A. (B) eV_{bb} for n-Si substrates grafted by a monolayer of **1**−**4**, derived from the data shown in Figure 8B.

due to the transfer of negative charges from p-Si to the molecules, giving rise to a weaker depletion in the space charge region.

For n-Si substrates, theoretically, the trends for E_{CBM} and its related eV_{bb} should be opposite to those for p-Si substrates when grafted with the same molecules. That is, Si−Mo samples exhibit the highest E_{CBM} and eV_{bb} for n-Si substrates, followed by Si−NO_2, then Si−NH_2, and Si−NMe_2 has the lowest E_{CBM} and eV_{bb}. This agrees very well with our experimental results (Figures 8B and 9B). Since the depletion layer in n-Si is induced by the negative surface charge (i.e., correlated with the positive space charge of ionized donors), the electron donating molecules give electrons to the n-Si substrates and, thus, become partly positively charged, resulting in a decrease in the negative surface charge density. Consequently, the depletion becomes weaker (lower eV_{bb}). Conversely, the depletion becomes stronger for the electron withdrawing molecules (higher eV_{bb}). Again, the trends are substrate independent.

Another method to determine the E_{VBM} for p-Si is to use the $E_{F,UPS}$ and HOMO (or E_{VB}) derived directly from UPS spectra

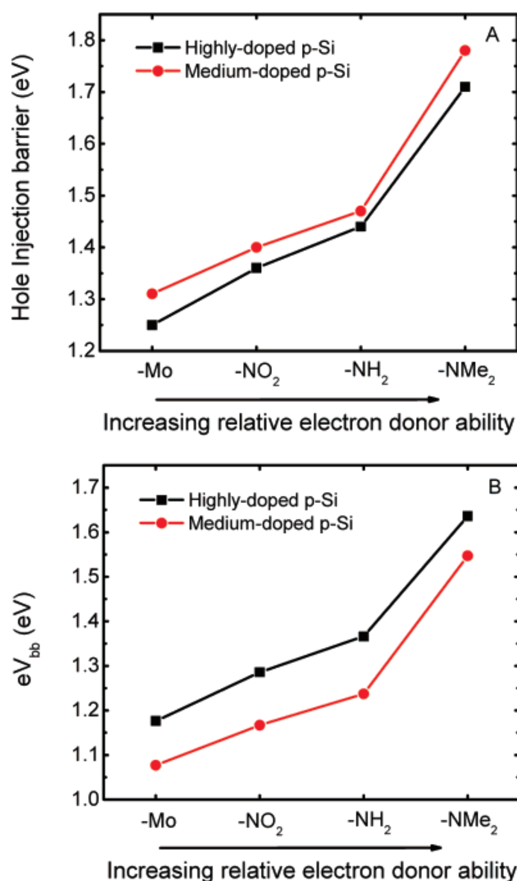

Figure 10. (A) Hole injection barrier of p-Si substrates grafted by a monolayer of **1**−**4** derived only from UPS data and (B) the related eV_{bb}.

and, thus, the corresponding eV_{bb} from eq 5. The results are shown in Figure 10, which displays an identical trend, albeit with different values, to the aforementioned ones resulting from the combination analysis using the data from both XPS and UPS/IPES. Theoretically, E_{CBM} can also be directly extracted using the $E_{F,IPES}$ and the LUMO (or E_{CB}) derived from the IPES spectra, and its related eV_{bb} can be calculated according to eq 6. However, the extracted maximal difference among the samples based on MD-n-Si substrates is 0.3 eV and that for samples based on HD-n-Si substrates is 0.2 eV. Considering the relatively low resolution of 0.6 eV for IPES characterization, the error for the extraction of E_{CBM} directly using IPES data is too high and, thus, it is not considered here although a trend similar to that derived from our other analytical techniques was observed. Furthermore, the height of the charge-transfer barrier can also be determined from the current−voltage curve[17] in which the charges pass through the molecules. However, we found that in our case, the barrier height derived from this method is similar for all the systems. This might result from the presence of pinholes and defects in the ultrathin molecular layers. Thus, these results will not be further discussed.

(d) Tailoring of Electron Affinity and Surface Potential Step Upon Molecular Grafting. χ at a semiconductor surface is defined as the energy required to excite an electron from the bottom of the E_{CB} at the surface to the local vacuum level.[39] That the molecular dipole can increase or decrease χ and WF is due to the presence of the electrical potential drop across the grafted molecular thin film, which is dependent on the dipole size and direction of the molecules attached on the surface; this

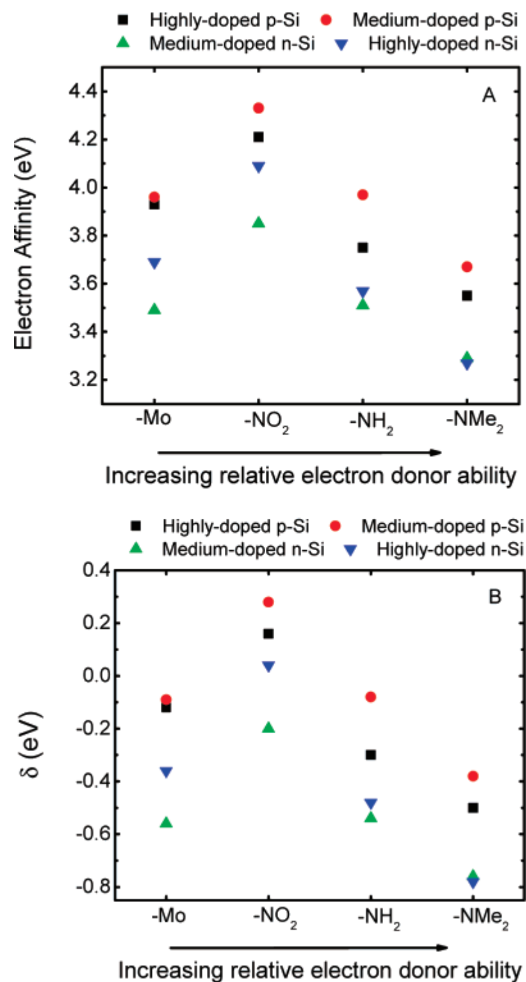

Figure 11. (A) Electron affinity of different Si substrates grafted by **1**−**4** and (B) the related surface potential step. The results are derived from the combination of XPS and UPS/IPES results.

can be extracted from the Helmholtz relation.[17,33,41] Provided the sign of the molecular dipole is defined to be negative if the positive pole of the dipole points away from the surface after grafting, attaching the molecules with a negative dipole will decrease the χ and WF because an emitted electron is accelerated within this dipole field on its way from the E_{CB} at the surface into the local vacuum. When attaching the molecules with a positive dipole, alternatively, the dipole field will impede the escape of electrons, resulting in an increase in χ and WF. In other words, for the same substrate surface the χ will be larger by grafting the molecules with a positive dipole than that with a negative dipole. The experimental observations (Figure 11A) are consistent with this theoretical prediction, which are derived combining the data from UPS/IPES and XPS, as indicated in eqs 9 (for n-Si substrates) and 10 (for p-Si substrates). The WF_{UPS} is obtained from UPS measurements as shown in the previous discussion. The E_{CBM} and E_{VBM} are derived as indicated in the previous section. The band gap of Si (E_g) is 1.12 eV. The molecules with a positive dipole (Si−NO_2) give rise to the highest χ, followed by Si−NH_2 (negative dipole), and the molecules with the most negative dipole (Si−NMe_2) result in the lowest χ. Because the molecule with Mo_6 cluster bears a positive dipole, it causes a higher χ than those with a negative

(41) Oliveira, O. N., Jr.; Taylor, D. M.; Lewis, T. J.; Salvagno, S.; Stirling, C. J. M. *J. Chem. Soc. Faraday Trans. 1* **1989**, *85*, 1009−1018.

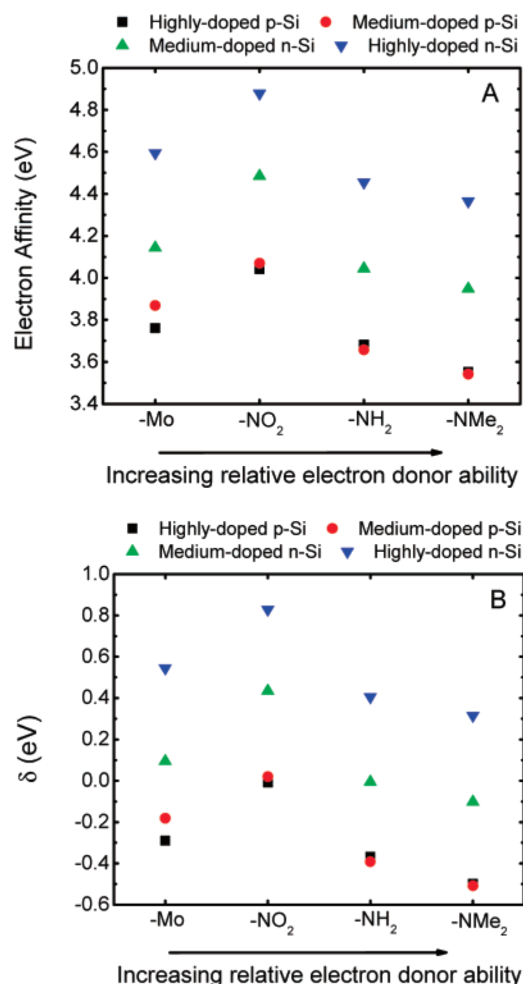

Figure 12. (A) Electron affinity of different Si substrates grafted by **1**−**4** and (B) the related surface potential step. The results are derived from Kelvin probe measurements.

dipole. Since the dipole size of the Mo_6 cluster molecule is unknown, it is not compared directly with Si−NO_2. Si−NO_2, Si−NH_2, and Si−NMe_2 are all approximately the same size, whereas Si−Mo is much larger, therefore only the first three are comparable in this trend. The contribution from the dipole moment of the grafted organic molecules to the work function of the studied surface is interpreted by surface potential step (δ), which is derived from eq 11 (4.05 eV for χ_{Si}). The same trend as that for χ has been observed (Figure 11B).

$$\chi_n = WF_{UPS} - E_{CBM} \quad (9)$$

$$\chi_p = WF_{UPS} + E_{VBM} - E_g \quad (10)$$

$$\delta = \chi - \chi_{Si} \quad (11)$$

χ and δ can also be determined using the Kelvin probe method in light of eqs 12 (for n-Si substrates) and 13 (for p-Si substrates) (Figure 12). The sum of the probe work function (WF_{KP}) and contact potential difference (CPD_L) can be considered as the work function of the investigated surface in the flat band condition when measured under photosaturation illumination. By means of the Kelvin method, the dipole effects of Si−C_6H_4−OCH_3 (negative dipole, but less negative than Si−C_6H_4−NH_2) and Si−C_6H_4−Br (positive dipole, but less positive than Si−C_6H_4−NO_2) were also determined. Both χ and δ were observed in the series Si−C_6H_4−NMe_2 < Si−C_6H_4−NH_2 < Si−C_6H_4−OCH_3 < Si−C_6H_4−Br < Si−C_6H_4−NO_2, which exhibits the same trends as those shown in Figure 11, although with different values, and is consistent with the sequence of the dipole moment and the relative electron donor ability of the grafted molecules. (In this discussion, we inserted −C_6H_4− for clarity with the newly viewed molecular systems.)

$$\chi_n = WF_{KP} + CPD_L - (E_{CB} - E_F) \quad (12)$$

$$\chi_p = WF_{KP} + CPD_L + (E_F - E_{VB}) - E_g \quad (13)$$

Sometimes the Si−NO_2 did not increase the electron affinity compared with that of bulk silicon (Figures 11 and 12), which is opposite to the aforementioned theoretical prediction. This is possibly caused by the presence of hydrogen adatoms on the surface for n-Si substrates. When compared with the n-Si bulk, an obvious decrease in electron affinity of the H-terminated n-Si surface was observed (Table 2). Considering that a complete termination of the Si surface with hydrogen adatoms is assumed to be obtained by BOE etching (~10^{15} cm^{-2}), whereas the molecular coverage is about 10^{13} cm^{-2}, a large amount of hydrogen adatoms still exist on the surface after molecular grafting and this is also observed in the surface IR.[27] Therefore, the presence of hydrogen adatoms will partly cancel the dipole effect from the grafted molecules with positive dipole moments. A stronger dipole moment effect was observed for the grafted molecules with negative dipole (Si−NH_2 and Si−NMe_2) than that for the H-terminated surface in both the literature[10] and our experiments, indicating the observed dipole effects (decrease in χ) in these systems are indeed from the grafted molecules. As for the p-Si substrates, however, the reason is still unclear since a slight increase in electron affinity was observed in the p-Si−H samples (Table 2). It is reported that the molecular dipole reduces due to the intermolecular dipole−dipole interactions when a monolayer is formed on a surface.[9] But our result for this case still cannot be fully explained since the dipole is always positive for **3** (Si−NO_2) even after molecular grafting; the electron affinity of the investigated Si−NO_2 surface should still increase as indicated in the previous discussion. Further research needs to be done to address this point.

(e) Charge Transfer and Dipole Moment Effects. The behavior of the Si−Mo system is explained by the following arguments. For the BE of Si2*p* core level and its related shift (Figures 3 and 4) and for E_{VBM} (E_{CBM}) and eV_{bb} (Figures 8, 9, and 10), the Si−Mo system is nearly located on the straight line of the trends for those values, whereas the Si−Mo system deviates from the trend for the WF and its related change (Figures 5 and 6) and for χ and δ (Figures 11 and 12). It is known from Figure 7 that the BE and E_{VBM} (E_{CBM}) vary with eV_{bb} and are measured or extracted with respect to the Fermi level, which are coherent in nature with the density and energy distribution of surface charges and are dependent on the charge transfer during the BOE etching and grafting process. When a molecule is covalently grafted directly to the surface, it is possible for fractional amounts of charge to transfer to or from the molecule, owing to its efficient interaction with the delocalized silicon wavefunctions. The amount and direction of the charge-transfer depends on many factors. The difference in the electronegativity between silicon and carbon atoms is not considered here since the same chemical bond is formed

among all the systems during the grafting process, although the electronegativity difference does influence the charge transfer. The difference in the work function or electrochemical redox potential between grafted molecules and silicon substrates also has an impact on the charge transfer. Depending on the size, polarity, and density, the dipole moment of the grafted molecule can cause charge redistribution within the system, leading to a change in the surface states and, thus, a change in the eV_{bb}. For an adsorbed single polar molecule, the substrate plays a major role in charge-transfer due to a dipole-induced dielectric response. Conversely, the molecules play the main role for an adsorbed monolayer because of the intermolecular dipole−dipole interactions.[9]

For the properties related to the eV_{bb}, therefore, the sequence in the trend of molecular effects results from a combination of the aforementioned factors. Among the samples grafted by **1**−**3**, the difference in the charge transfer must be due to the presence of the different functional groups, since that is the only difference in the structures and components among them (assuming the same molecular coverage for them due to their similar footprint size). As we have discussed, the p-Si substrate grafted by the molecules with the strongest electron donating capacity (the Si−NMe_2 system) exhibits the highest eV_{bb}, while the one with the strongest electron withdrawing group (Si−NO_2 system) has the lowest eV_{bb}, and the value for Si−NH_2 is located between them. For n-Si substrates, the trend for molecular effects on the eV_{bb} is in the opposite order. Regardless of the type of substrates, grafting of the molecules with −NMe_2 groups (the most electron-rich molecules) make the silicon more n-type, the ones with −NH_2 (less electron-rich molecules) make it again more n-type but not as much as with the −NMe_2, and the molecules with −NO_2 (electron-deficient molecules) make it more p-type (Figures 3 and 4).

As for the Si−Mo system, the size of its footprint is much larger than in the other cases, resulting in a lower molecular monolayer coverage. Therefore, it is unreasonable to compare the dipole moment effects of the Si−Mo directly with the other shorter systems. Considering nitrobenzene has a more negative reduction potential than that of the aryl polymolybdate cluster,[42−44] the substrates can gain less negative charge or more positive charge from Si−Mo than that from Si−NO_2. For p-Si substrates, therefore, the Si−Mo system exhibits a lower eV_{bb} (weaker depletion) than Si−NO_2, whereas for n-Si substrates the Si−Mo system leads to a higher eV_{bb} (stronger depletion) than Si−NO_2. Thus, the work function and electrochemical redox potential of the grafted molecules are playing a role in the change of eV_{bb}, i.e., both the low eV_{bb} for p-Si substrates and high eV_{bb} for n-Si substrates are mainly caused by the less-negative reduction potential of the aryl polymolybdate cluster. Due to the same effects, regardless of the type of substrates, grafting of the Mo_6 cluster made the silicon more p-type than the molecules grafted with −NO_2 (Figures 3 and 4). These afford evidence that, as well as the dipole moment, the redox potential or work function of the grafted molecules should also be considered as a factor that can influence the charge transfer. In addition, for H-terminated substrates (Si−H), a relatively high eV_{bb} was observed for both p- and n-Si substrates (Table 2). Since the molecular coverage for Si−Mo is much lower than that for the other molecule types, more hydrogen adatoms are present on the surface of the Si−Mo sample. This combination of factors account for the observed experimental phenomena.

Table 3. Values of Energy Levels for the Samples of Silicon Covered Only by Oxides (eV)

	$BE(Si2p_{3/2})^a$	WF^b	$E_{VBM}{}^c$	$E_{CBM}{}^c$	$eV_{bb}{}^c$	χ^b	δ^b
HD-p-Si	99.09	4.82	0.40		0.327	4.02	−0.03
MD-p-Si	99.38	4.84	0.65		0.387	4.39	0.34
MD-n-Si	99.44	4.88		0.86	0.605	4.35	0.30
HD-n-Si	99.62	4.79		0.65	0.632	4.84	0.79

[a] The values are derived from XPS. [b] The values are from Kelvin probe measurements. [c] The values are from the combination of XPS and UPS/IPES results.

Alternatively, the determination of WF and χ is related to the surface potential step (δ), which is dependent on the dipole moment of the grafted molecules. As discussed above, attaching the molecules with positive dipole increases the WF, χ, and δ, regardless of the type of silicon (n- or p-), whereas grafting the molecules with negative dipole results in a decrease of the values. According to the experimental results (Figures 11 and 12), the dipole effects in Si−Mo are less than those in Si−NO_2 but stronger than Si−NH_2. Since the molecular coverage and package density of Si−Mo are different from the other smaller molecules, it is not reasonable to compare it directly. In addition, because of the intermolecular dipole−dipole interactions (for an adsorbed molecular layer) or dipole-induced dielectric response (for an adsorbed single polar molecule) and/or the charge transfer between the grafted molecules and silicon substrates, the dipole moment of the grafted molecules may be different from that prior to grafting. If the same molecules are used, then different doping types and densities in silicon substrates can lead to different amounts of charge transfer between the grafted molecules and silicon, resulting in different dipole moments of the grafted molecules and, thus, in different δ. This may explain the observed phenomenon wherein there is a relatively large spread in χ and δ when the same molecules are grafted onto different substrates.

SiO_x is formed on the surface of the grafted samples due to an unintended oxidation during the grafting process, which is also observed via electrochemical grafting.[10] For p-Si substrates, the samples covered only by oxides have a low eV_{bb} while for n-Si substrates the eV_{bb} is high (Table 3). The defects associated with oxide formation are the presumed reason for the eV_{bb}. For both n- and p-Si substrates, an increase in electron affinity was observed for the samples completely covered by oxides compared with that of bulk silicon (Table 3).[45] However, the surface oxide overall contribution should be very low since the amount of oxides on the surface is much less than that of grafted molecules and hydrogen adatoms. In addition, the eV_{bb} for highly doped n- or p-Si substrates appears to be slightly high. This is attributed to the presence of Si−H and/or oxide on the surface. Another possible reason may come from its more metal-like properties for highly doped silicon substrates, which makes the charge-transfer much easier.

(42) Lu, M.; Xie, B.; Kang, J.; Chen, F.; Yang, Y.; Peng, Z. *Chem. Mater.* **2005**, *17*, 402−408.
(43) Donkers, R. L.; Workentin, M. S. *Chem. Eur. J.* **2001**, *7*, 4012−4020.
(44) Kang, J.; Nelson, J. A.; Lu, M.; Xie, B.; Peng, Z.; Powell, D. R. *Inorg. Chem.* **2004**, *43*, 6408−6413.

(45) The only exception is for the HD-p-Si covered by oxides. However, considering that the measurement error for the Kelvin probe is at least several meV, −0.003 eV for the difference in the electron affinity is within the error.

Conclusions

On the basis of the results presented here, the electronic structures (WF, E_{VBM} (E_{CBM}), eV_{bb}, χ, and δ) of the Si/molecule interface can be tuned systematically in accordance with the electron donating ability, redox capability or work function, and/or dipole moment of the grafted molecules. The molecular effects result in a change both in eV_{bb} (charge transfer) and in electron affinity (dipole moment) of the studied surfaces. Although the absolute values for these physical parameters are difficult to determine, the investigated samples provide an internally consistent set for relative comparisons, which is preferred and suitable for analysis. Although the influences from residual hydrogen adatoms and unintended oxides on the surface should be considered, the electrostatic behavior of the nonperfect molecular monolayer is still significant enough for the modulation of electronic structures. The results could have practical implications for (bio)sensors and, especially, for controllable tuning of electronic performance in nanosized devices via surface engineering where consistent impurity doping using traditional doping techniques is difficult to achieve, whereas surface modifications become attractive at the nanoscale since the surface-to-volume ratio increases dramatically.

Acknowledgment. DARPA/ARL provided funding for the work at Rice. The work at University of Rochester is supported in part by NSF DMR-0602870.

JA0768789